THE JOURNAL OF PHYSICAL CHEMISTRY Letters

Perspective

Cite This: J. Phys. Chem. Lett. 2018, 9, 3946–3958

pubs.acs.org/JPCL

Building Next-Generation Li-ion Capacitors with High Energy: An Approach beyond Intercalation

Vanchiappan Aravindan*,† and Yun-Sung Lee*,‡

†Department of Chemistry, Indian Institute of Science Education and Research (IISER), Tirupati 517507, India

‡Faculty of Applied Chemical Engineering, Chonnam National University, Gwang-ju 500-757, Republic of Korea

ABSTRACT: Hybridization of two prominent electrochemical energy storage systems, such as high-energy Li-ion batteries and high-power supercapacitors into a single system, tends to deliver high-energy and high-power capabilities; such systems are often called Li-ion capacitors (LICs). The utilization of battery-type electrodes, which undergo a traditional intercalation process, in LICs provides the necessary energy; however, their limited reversible capacities and higher redox potentials (except graphite and hard carbon) hinder achieving high values. Using materials that can undergo either alloying or conversion or both together with Li, rather than intercalation, is an attractive approach to achieve high energy without compromising both power capability and cyclability. This Perspective discusses the possibility of using high-capacity, exhibiting relatively lower redox potential than transition metal-based intercalation hosts, low-cost materials in conversion and alloying reactions with Li, along with prelithiation strategies (Aravindan, V.; Lee, Y.-S.; Madhavi, S. Best Practices for Mitigating Irreversible Capacity Loss of Negative Electrodes in Li-Ion Batteries. *Adv. Energy Mater.* **2017**, *7*, 1602607). Future prospects on working with alloying and conversion-type materials are discussed in detail.

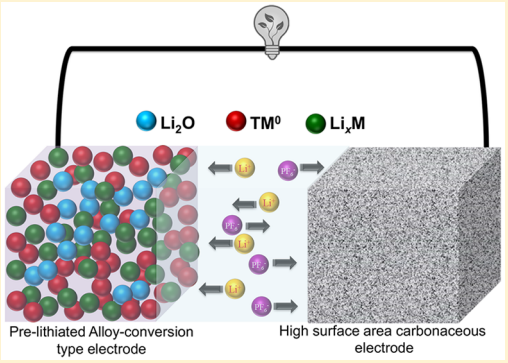

Li-ion hybrid electrochemical capacitors or Li-ion capacitors (LIC) have gained much attention in the recent past owing to their high energy densities compared to conventional supercapacitors, i.e., electric double layer capacitors (EDLCs), and higher power capability than Li-ion batteries (LIBs).[2−8] Although moderate energy and power capability are noted for LICs, their performance is still inferior for high-end applications, such as hybrid electric vehicles (HEVs) and electric vehicles (EVs). Tailor-made high surface area activated carbon (AC) has been predominantly used as the EDLC component in LIC assemblies, but the enhancement in energy is limited, as it undergoes only non-Faradaic charge storage. Similarly, battery-type components (insertion-type anodes, e.g., metal oxides and phosphates) also experience kinetic limitations, and a high intercalation potential severely dilutes the net energy density of the system. As a result, the energy density of a LIC is limited to <100 Wh kg^{-1}. Achieving an energy density >100 Wh kg^{-1} is possible when prelithiated graphite or hard carbon (HC) is used as an insertion-type component in LICs.[9,10] Graphite exhibits better cyclability but its inferior electrochemical activity at high currents is a serious issue.[11−13] HC is an important alternative for graphite in terms of high current performance, but its Li-insertion potential is slightly higher (>0.2 V vs Li); further, its limited cycle life when compared to graphite is an issue. This is mainly because of the randomly arranged/oriented graphitic planes embedded in the amorphous carbon matrix.[14] Nevertheless, both prelithiated graphite and HC deliver good electrochemical performance in LICs; on the other hand, they struggled to meet the standards required for the aforesaid HEVs and EVs.

In this context, research attention is being concentrated toward the development of high performance battery components to achieve high energy densities without compromising the power density within the limited thermodynamic stability window of conventional carbonate-based solutions. Apart from insertion-type anodes, conversion/displacement and alloy-type anodes are also being explored to overcome capacity limitations and power capabilities of carbonaceous anodes in LIBs.[11,15] However, conversion-type anodes have limited scope in the LIB industry owing to the huge polarization they undergo, apart from irreversibility and volume variation issues. Although less polarization is noted for alloy-type anodes, stability remains an issue owing to the unusual volume variation during the alloying/dealloying reactions.[11,16] On the other hand, the irreversibility and volume variation issues can be efficiently tackled, for example, by pretreating the electrode to mitigate irreversibility and using hollow-structured active materials or making composites with carbonaceous counterparts. Polarization is an intrinsic feature of the individual materials and hence it cannot be easily overcome during device fabrication. On the other hand, LIC has a wider potential window; hence the usage of high capacity conversion- and alloy-type materials along with high surface area carbonaceous materials is possible, and high energy densities can be realized. Graphite or HC requires prelithiation before a LIC is fabricated, whereas a

Received: May 1, 2018
Accepted: June 28, 2018
Published: July 5, 2018

DOI: 10.1021/acs.jpclett.8b01386
J. Phys. Chem. Lett. 2018, 9, 3946–3958

conversion- or alloy-type anode could be treated in the same fashion for one or two cycles to eliminate irreversibility.[17,18] In contrast to insertion-type carbonaceous hosts, a variety of compounds are available, hence, based on the metallic reduction (M^0) or alloying potential, the testing window and high power capabilities of LICs can be tailored. This clearly suggests that various aspects of the alloying and conversion materials used in LICs have to be discussed elaborately. In this regard, the current study presents a complete overview of the research in progress on the fabrication of high-energy LICs using conversion- and alloy-type anodes (Scheme 1). The future prospects of these materials are also discussed.

Scheme 1. (a) Schematic Illustration of a Typical Li-Ion Capacitor[a]; (b) Schematic Representation of the Electrode Potentials versus Specific Capacity for EDLC (Pink Lines) and Li-Insertion Electrodes Like $Li_4Ti_5O_{12}$ and LiC_6[b]

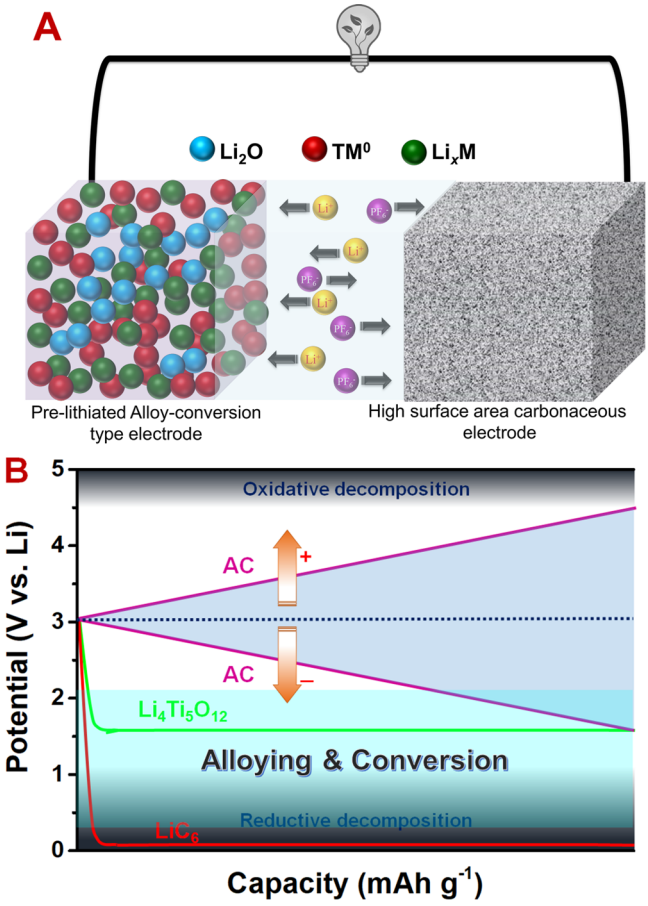

[a]Green – Li_xM alloy; red – transition metal (M^0), and blue – Li_2O matrix. [b]The redox potential of the alloying and conversion anodes are highlighted.

In general, an alloy is described as a mixture of two or more elements. Alloy formation is completely reversible during an electrochemical charge–discharge process (Scheme 2). The motivation behind exploring such alloy-based materials, especially with Group IV elements (Si, Ge, Pb, and Sn), is mainly based on their high theoretical capacity (>600 mAh g^{-1}) and low working potential (<1 V vs Li) compared to transition metal-based insertion and conversion-type anodes.[11,13,19,20] As mentioned earlier, the large irreversibility and volume variation are the main issues that adversely affect the

Scheme 2. Typical Alloying/Dealloying Reactions of (A) Pure Metals with Li, (B) Metal Oxides, and (C) Ternary Oxides in Which, Besides the Alloying Reaction of Metal with Li, Oxidation of Such Transition Is Also Possible (Conversion Mechanism)

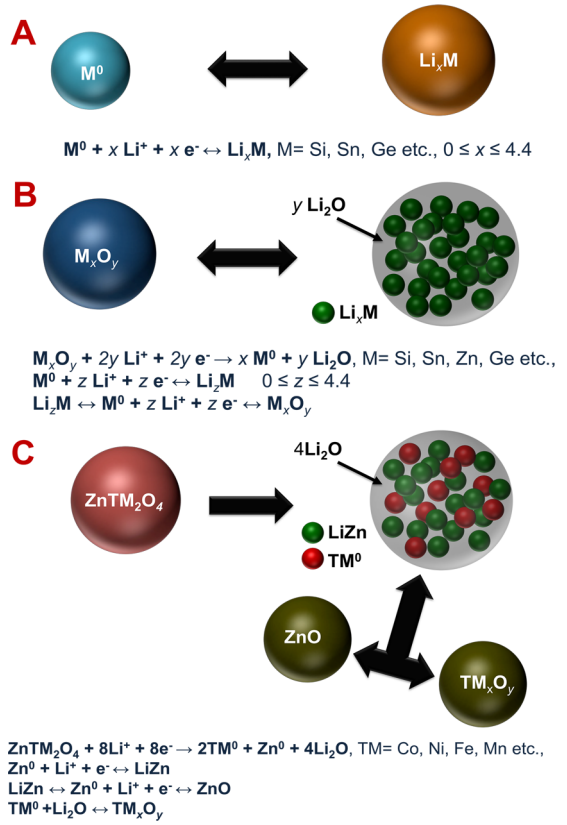

electrochemical profiles of alloy-type anodes and eventually lead to the cracking and detaching of active particles (i.e., pulverization of the electro-active particulates) from the current collector.[16] Hence, composites of carbonaceous materials with either active or inactive matrix elements are suggested to counter the volume variations. Further, the preparation of hollow-structured materials is another possible aspect to improve the electrochemical activity of such alloy-type negative electrodes.

Si is a Group IV element extensively studied as a potential electrode material for LIBs. Si exhibits several advantageous features, such as a low working potential (<0.3 V vs Li), high volumetric capacity (~9786 mAh cm^{-3}), and gravimetric capacity (~3579 mAh g^{-1}); furthermore, it is more abundant in the earth's crust. Interestingly, the theoretical capacity of $Li_{15}Si_4$ is very close to that of metallic Li (~3862 mAh g^{-1}). Thus, a number of research studies have been carried out on this anode material.[21−27] The electrochemical activity of Si can be described as shown below.

$$\text{During discharge:}\quad \text{Si (crystalline)} + x\text{Li}^+ + xe^- \rightarrow \text{Li}_x\text{Si (amorphous)} + (3.75 - x)\text{Li}^+ + (3.75 - x)e^- \rightarrow \text{Li}_{15}\text{Si}_4\ \text{(crystalline)}$$

$$\text{During charge:}\quad \text{Li}_{15}\text{Si}_4\ \text{(crystalline)} \rightarrow \text{Si (amorphous)} + y\text{Li}^+ + ye^- + \text{Li}_{15}\text{Si}_4\ \text{(residual)}$$

DOI: 10.1021/acs.jpclett.8b01386
J. Phys. Chem. Lett. 2018, 9, 3946−3958

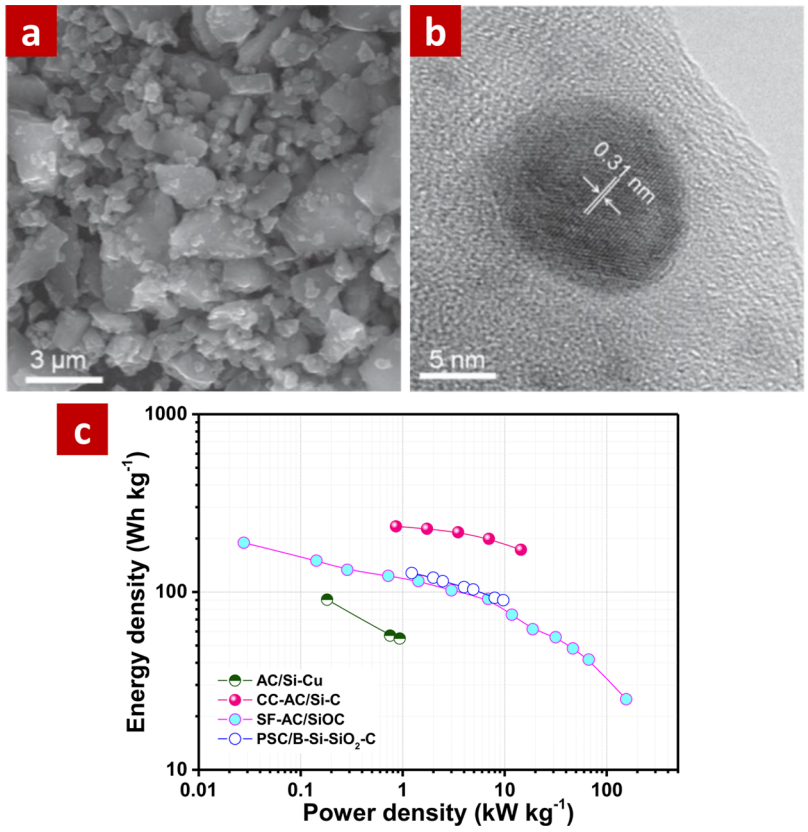

Figure 1. (a) Scanning electron microscope (SEM) image of B−Si−SiO_2−C. (b) High resolution transmission electron microscope (HR-TEM) image of B−Si−SiO_2−C. Reproduced with permission from ref 33. Copyright 2014, John Wiley and Sons. (c) Ragone plot of LICs based on different Si-based active materials, including AC/Si−Cu dome,[32] SF-AC/SiOC,[39] CC-AC/Si−C,[34] and PSC/B−Si−SiO_2−C[33]

Unfortunately, the solid electrolyte interphase (SEI) formation mechanism over a Si anode is completely different from that on carbonaceous anodes, specifically graphite; further, the interphase is unstable as well. The aggregation of Si nanoparticles observed during the charge process owing to the welding effect is believed to be responsible for the fading capacity as well as the unstable SEI formation.[28,29] Therefore, Si-based anodes must be prepared with either a carbonaceous matrix or active/inactive matrix elements. The presence of carbonaceous content confers a stable surface film-forming ability to the composite; moreover, the unusual volume variations upon alloying/dealloying can be sustained. On the other hand, the utilization of hollow-structured materials is also preferred, as they can sustain volume variations up to a certain level.[30] Among the Group IV elements, volume variations are very large in the case of Si (434% and 399% variation in the volume for amorphous and crystalline phases, respectively). Interestingly, the electrochemical activity of thin films, powers with amorphous or crystalline nature, exhibits different profiles. Hence, it is very difficult to compare the electrochemical activities of different phases. Saito et al.[31] studied the influence of additives (vinylene carbonate and fluoroethylene carbonate (FEC)) and vacuum pressure impregnation (VPI) on the electrochemical activity of commercial Si nanoparticles. VPI certainly led to better and stable electrochemical activity owing to the homogeneous distribution of active materials and allowed the complete participation of the Si nanoparticles in the reaction. Irrespective of the presence or absence of additives, prelithiated Si nanoparticles exhibited excellent cycling profiles in a half-cell assembly. In particular, FEC-based solutions displayed better electrochemical characteristics. Further, the same behavior is observed in LICs when paired with AC. The LICs delivered a maximum energy density of ∼114 Wh kg^{-1}, but no cycling profile is presented to ensure the long-term stability. In this regard, Liu et al.[32] reported the fabrication of Cu−Si dome patterned electrodes as negative electrodes for a LIC assembly with AC and compared them with conventional Cu−Si composites. The dome patterned electrodes are prepared by a two-step process; likewise, first Cu-patterning over polylactic acid template covered Cu substrate is achieved via electroplating. Subsequently, Si is patterned on the Cu substrate by electron cyclotron resonance chemical vapor deposition. The conventional Cu−Si electrodes are not precycled or lithiated before being coupled with AC in the LIC assembly. Prelithiated Cu−Si domes showed an initial discharge capacity of ∼3500 mAh g^{-1}. Accordingly, the mass ratio between Cu−Si domes and AC is fixed at 1:10. The AC/Cu−Si dome-based LIC delivered a maximum energy density of ∼90 Wh kg^{-1} in the 2.2−3.8 V region. Further, an excellent cyclability of over 15 000 cycles is noted without any fading in the case of Cu−Si dome-based LICs, whereas a drastic fading is observed with conventional Cu−Si-based composites. Yi et al.[33] suggested the possibility of using a boron-doped Si composite as a negative electrode (B−Si−SiO_2−C) for LICs. These composite electrodes delivered a stable reversible capacity of ∼1279 mAh g^{-1} after 100 cycles. The mass loading between the porous spherical carbon (PSC) and the B−Si−SiO_2−C composite is adjusted to a 2:1 ratio. Accordingly, the LIC is constructed using prelithiated B−Si−SiO_2−C as the negative electrode and PSC as the positive terminal. This LIC

DOI: 10.1021/acs.jpclett.8b01386
J. Phys. Chem. Lett. 2018, 9, 3946−3958

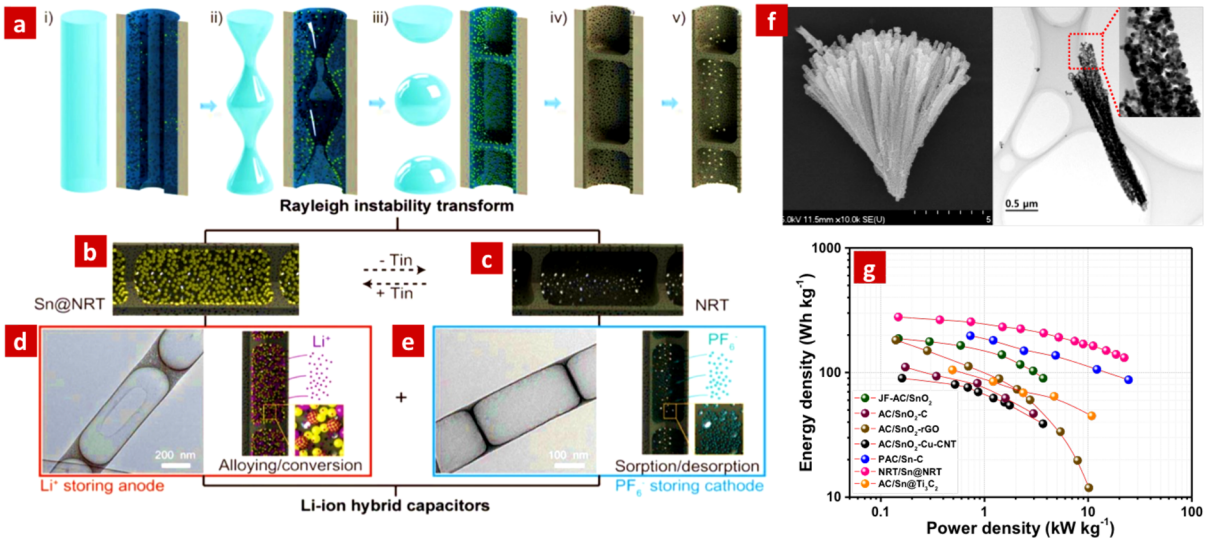

Figure 2. Overall procedure for the design of nitrogen-rich nanotubes (NRTs) for hybrid capacitors. (a) Fabrication of NRTs using both hard and soft templates, which include (i) a process for the controlled synthesis of the external morphology using Melamine−Formaldehyde resins and surfactants (F127) in the hard template, (ii,iii) processes for the controlled synthesis of the NRT with connected internal compartments, which are formed via the Rayleigh instability transform, and (iv,v) processes to produce an internal compartment with open mesoporous channels via the carbonization of melamine−formaldehyde resins and surfactants, followed by the removal of the hard template. Schematic illustration of (b) Sn@NRT and (c) NRT. Morphology of (d) Sn@NRT and (e) NRT structure with a schematic illustration showing the ion penetration processes. Reproduced with permission from ref 44. Copyright 2016, John Wiley and Sons. (f) Morphological features of SnO_2 nanobundles. Reproduced with permission from ref 45. Copyright 2017, Elsevier. and (g) Ragone plot of the LICs based on various Sn-based active materials, including JF-AC/SnO_2,[45] AC/SnO_2−C,[46] AC/SnO_2-rGO,[48] AC/SnO_2−Cu-CNT,[47] PAC/Sn−C,[43] NRT/Sn@NRT,[44] and AC/Sn@Ti_3C_2.[50]

is capable of delivering a maximum energy density of ∼128 Wh kg^{-1} in the 2−4.5 V range. In this potential range, the capacity retention is inferior (∼70%) compared to the narrow potential window of 2−4 V (∼77%). A Si-based composite (Si−C) anode with a corncob derived AC (CC-AC) in a LIC assembly is reported by Li et al.;[34] these anodes are reported to yield high energy density. Authors procured commercially available Si particles (MTI Corp.) as active materials and subsequently carbon-coated them by decomposing acetylene. On the other hand, the CC-AC is activated chemically using KOH (3:1 ratio) in a NH_3/N_2 atmosphere to yield a N_2-doped AC. CC-AC treated at 400 °C exhibits high specific surface area (∼2859 m^2 g^{-1}) and capacitive property (∼182 F g^{-1}) with Li. In this case, FEC (10%) is used as an additive along with a conventional electrolyte (1.2 M $LiPF_6$ in EC:DEC:DMC (1:1:1 v/v/v)), in order to stabilize the Si-based system upon long-term cycling.[35−37] This CC-AC/Si−C system displayed a maximum energy density of ∼238 Wh kg^{-1} in the 2−4.5 V range; the energy density experienced a decrease (∼169 Wh kg^{-1}) in a narrow potential window (2−4 V). Furthermore, an excellent cyclability of 8000 cycles is noted with a retention of ∼88% in the narrow potential window. The same research group explored the possibility of using egg white-derived porous carbon with a prelithiated Si−C composite anode in a LIC assembly; an energy density of ∼257 Wh kg^{-1} could be achieved with such a system.[38] Furthermore, an enhanced cyclability is noted; for example, ∼79.2% capacity is registered after 15 000 cycles in the 2−4.5 V range. As expected, when the upper cutoff potential is reduced to 4 V, the cycling performance increased to ∼86%. Halim et al.[39] explored low-carbon silicon oxycarbide (LC-SiOC) as a negative electrode for LIBs and LICs; an LIC is fabricated along with snake fruit-derived AC (SF-AC). SiOC is derived from conventional silicone oil at various calcination temperatures. The SiOC sample derived at 900 °C yielded a high-performance material. Later, the same SiOC is prelithiated by internal short-circuiting and paired with SF-AC. The LIC incorporating this LC-SiOC delivered a maximum energy density of ∼200 Wh kg^{-1} along with an ultrahigh power capability of 156 kW kg^{-1} (Figure 1). Interestingly, over 97% of the initial energy density is retained in the 1.5−4 V range after 40 000 cycles, which is one of the most remarkable results reported on alloy-based anodes in LIC assemblies.

Pure Sn metal is considered as one of the promising negative electrode for LIBs.[11] Interestingly, a Sn-based composite, Sn−Co−Ti-C, has been commercialized by Sony in the Nexelion configuration along with a mixed layered oxide cathode.[40,41] Similar to Si, Sn (in the form of $Li_{4.4}Sn$) also exhibits promising characteristics, such as a low redox potential (∼0.3 V vs Li), high density (∼7.3 g cm^{-3}), and high theoretical capacity in gravimetric (∼993 mAh g^{-1}) and volumetric (7241 mAh cm^{-3}) scales.[42] It is well-known that Sn undergoes an alloying reaction with Li according to the following reaction, $Sn + 4.4Li^+ + 4.4e^- \leftrightarrow Li_{4.4}Sn$. Unfortunately, similar to Si anodes, large unit cell volume variations (∼259% for the crystalline phase and ∼305% for the amorphous phase)[19] are the main concern with Sn anodes during alloying/dealloying reactions. Therefore, Sn-based materials require a buffer matrix (either active or inactive) to sustain such variations. Indirectly, this requirement indicates that anodes in the composite form are superior to those in the native form, in terms of cyclability and high reversible capacity. In this regard, Sun et al.[43] reported rationally designed Sn−C composites as negative electrodes with pomelo peel-derived AC (PAC) as the cathode. In this approach, Sn−C is prepared by infiltrating a N-rich porous carbon framework with a $SnCl_2$ solution; the framework is subsequently subjected to calcination. Very high reversibility, higher even than the theoretical capacity, is noted

DOI: 10.1021/acs.jpclett.8b01386
J. Phys. Chem. Lett. 2018, 9, 3946−3958

for the Sn−C electrode in a half-cell configuration. This electrode has also been prelithiated and paired with a PAC obtained at 900 °C. Interestingly, the LIC has been tested for maximum extent up to 4.5 V. This eventually leads to a high energy density of 195.7 Wh kg^{-1} with excellent cycling profiles of 70% retention after 5000 cycles. Won et al.[44] reported the fabrication of Sn encapsulated N-rich nanotubes (Sn@NRT) as negative electrode and NRTs as cathode. The tube-like structure sustains the volume variations observed during the alloying process owing to its robustness, during the half-cell performance over 3000 galvanic cycles. The LIC assembly has been tested in the range of 1.75 to 4.35 V and delivered an energy density of ∼274 Wh kg^{-1} with an exceptional cycling profile (3000 cycles) with 80% retention. Marine algae-inspired SnO_2 nanobundles have been reported as negative electrode for the fabrication of high energy LICs with jack fruit skin-derived AC (JF-AC).[45] The prepared SnO_2 was composed of mixed phases, such as the tetragonal phase (87.1%) and the orthorhombic phase (12.83%). Further, attempts have been made to optimize the conducting carbon concentration and various electrolyte solutions in the restricted testing range up to 0.8 V vs Li to improve the electrochemical activity of SnO_2 in a half-cell assembly. This potential window allows the active material to buffer only for the alloying reaction ($Li_{4.4}Sn \leftrightarrow Sn^0 + 4.4Li^+ + 4.4e^-$), but not for the conversion of its oxide (SnO and SnO_2). Under the optimized conditions, the prelithiated SnO_2 and JF-AC delivered a maximum energy density of ∼187 Wh kg^{-1} in the 1.7−4.2 V window with ∼82% retention after 10 000 cycles. Similarly, the influence of carbon concentration on SnO_2−C hybrid systems is also studied, in which both high (75%) and low (40%) carbonaceous composites exhibited inferior electrochemical activities compared to the activity at an optimal loading of ∼57%.[46] A spontaneous lithiation procedure is adopted for the prelithiation process. Accordingly, the optimized loading-based LIC delivered an energy density of ∼110 Wh kg^{-1} in the 0.5−4 V range with ∼80% retention after 2000 cycles. Hsieh et al.[47] attempted to use SnO_2−Cu−CNT-based composite electrode for the fabrication of LICs with commercial AC by altering the anode to cathode ratio. However, a more or less similar performance is observed for the assembly irrespective of the loading ratio; an energy density of ∼90 Wh kg^{-1} could be delivered with 3.8 V window. Similarly, a SnO_2-rGO composite is also reported along with commercial AC and it exhibits a very high energy density of ∼186 Wh kg^{-1} (Figure 2).[48] However, cycling profiles, which indicate the long-term stability of the prepared rGO-based composite, have not been reported. Recently, MXenes gained special attention owing to their layered structure, which can accommodate a wide range of foreign cations, such as Li^+, Na^+, K^+, Mg^{2+}, NH^{4+}, and Al^{3+} as well as some small organic molecules to produce intercalation compounds with fascinating properties and multifarious applciations.[49] Intercalation compounds are predominantly used as host matrices in rechargeable batteries, specifically LIBs. In this context, Luo et al.[50] reported the possibility of using Sn(IV)-intercalated Ti_3C_2 via a cetyltrimethylammonium bromide-assisted process ($Sn@Ti_3C_2$). In this case, Sn undergoes an alloying reaction with Li, whereas the layered Ti_3C_2 undergoes a typical intercalation process. This combined heterogeneous charge storage process yields very high reversibility of over 500 mAh g^{-1} in a half-cell assembly. Unlike other conventional intercalation hosts, the $Sn@Ti_3C_2$ composite experiences a huge irreversible capacity loss (ICL). This is mainly because of the alloying reaction of Sn with Li. In order to overcome the ICL issue, test cells are fabricated and cycled for 10 cycles, and prelithiated before being paired with an AC. Such a cell delivered a maximum energy density of ∼106 Wh kg^{-1} within a restricted testing window of 1−4 V. However, fading is observed in the cycling profiles. For example, only ∼71% of initial energy density is retained after 4000 cycles. The Ragone plot clearly suggests that the pure metal and its composites are capable of achieving higher values than the oxide form (e.g., SnO_2). This is mainly because of the formation of an electrically insulating amorphous Li_2O phase during the first discharge process; on the other hand, Li_2O was not formed in the case of Sn and its composites with carbonaceous counterparts, such as CNTs, rGO, and C (Scheme 2B).

Conversion (often called "displacement") is a reversible process, in which the structure of the compound (M_yX_z, M = metal, X = P, S, O, F, Cl, etc.) is destroyed electrochemically and eventually reduced to metallic nanoparticles (M^0) in a buffer matrix, such as Li_2O, Li_2S etc. Theoretically, upon charging, the electrochemically reduced metallic nanoparticles regain their original state (M_yX_z) (Scheme 3). Due to the

Scheme 3. Li-Storage Mechanism via Conversion Reaction

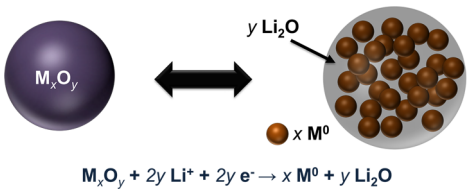

multiple electron reactions, conversion-type electrodes can deliver higher reversible capacity than insertion-type materials such as graphite.[11] Unavoidable electrolyte decomposition occurs in the first cycle similar to the alloying-type materials. This eventually leads to the formation of a SEI layer which is predominantly composed of insoluble inorganic byproducts. As a result, a huge ICL is noted in the first cycle as compared to graphite. It is worth mentioning that the chemical composition of the SEI layers formed over the conversion anodes are different from those formed on graphitic anodes. Apart from this, the huge polarization, volume variation, and poor cyclability characteristics are other issues that need to be tackled with this kind of anodes. The formulation of a composite or coating with carbonaceous materials/passive elements is proposed to sustain volume variations and to subsequently improve stability upon cycling. Prelithiation of the electrode is generally performed before employing it as a negative electrode in a LIC. Nevertheless, the large polarization characteristic of such conversion electrodes certainly forbids their potential use in secondary battery applications. On the other hand, LICs operate in a wider potential window; therefore, such conversion-type materials could be efficiently used as promising negative electrodes if their polarization effects can be ignored.

Iron oxides are one of the most important conversion-type anodes explored for LIB applications owing to their high theoretical capacity (∼1008 mAh g^{-1} for hematite, $Fe_2O_3 + 6Li^+ + 6e^- \leftrightarrow Fe^0 + 3Li_2O$ and ∼926 mAh g^{-1} for magnetite, $Fe_3O_4 + 8Li^+ + 8e^- \leftrightarrow Fe^0 + 4Li_2O$), low cost, and eco-friendly characteristics. They also exhibit a low reduction potential of ∼0.7 V vs Li. In this regard, Zhang et al.[51] reported the formulation of a Fe_3O_4-graphene composite (Fe_3O_4-G) using

DOI: 10.1021/acs.jpclett.8b01386
J. Phys. Chem. Lett. 2018, 9, 3946−3958

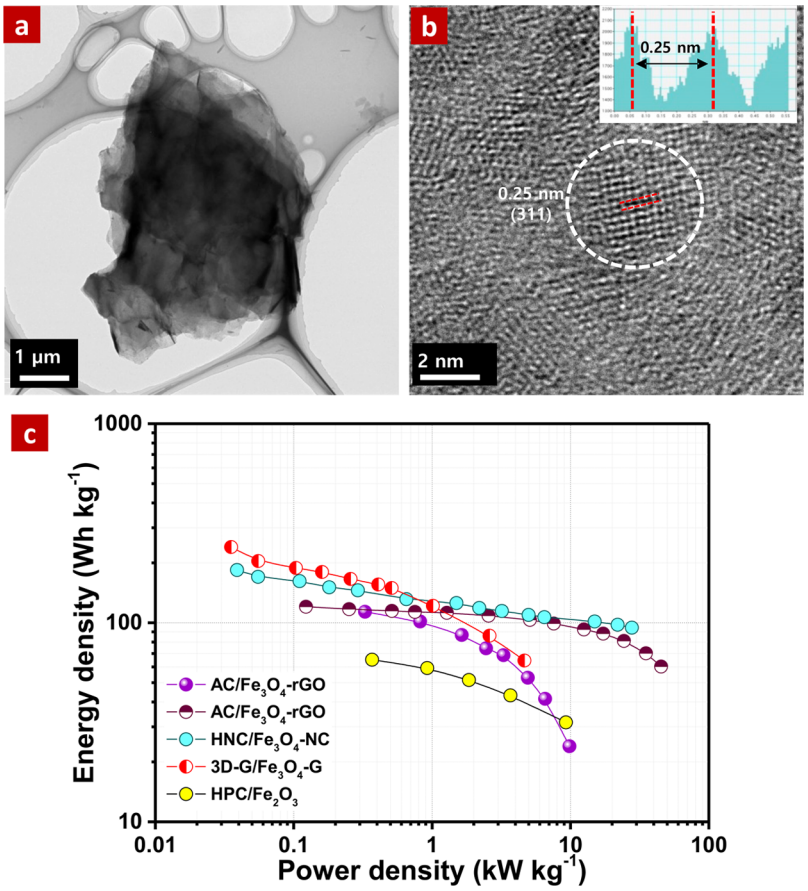

Figure 3. (a) TEM images of Fe_3O_4-rGO, (b) HR-TEM images of the same materials at 1 500 000× magnification. The inset shows the corresponding lattice plane distances of as-prepared magnetite nanoparticles. Reproduced with permission from ref 53. Copyright 2017, John Wiley and Sons. (c) Ragone plot of the LICs based on various Fe-based active materials, including 3D-G/Fe_3O_4-G,[51] AC/Fe_3O_4-rGO,[52] AC/Fe_3O_4-G,[53] HNC/Fe_3O_4−NC,[54] and HPC/Fe_2O_3@C.[55]

an *in situ* solvo-thermal approach. Graphite oxide is hydrothermally treated with sucrose and subsequently activated with KOH to yield a porous 3D graphene (3D-G) counter electrode with a surface area of ∼3355 m^2 g^{-1}. The Fe_3O_4-G electrode delivers a reversible capacity of ∼1089 mAh g^{-1} at low current rates (0.1 C) with good cyclability in a half-cell assembly. A LIC fabricated with precycled Fe_3O_4-G as the negative electrode (no prelithiation) and a 3D-G counter electrode delivered a maximum energy density of ∼240 Wh kg^{-1} at the optimized mass loading. However, fading is noted in the cycling profiles; for example, only ∼70% of the initial energy density is noted after 1000 cycles. Zhang et al.[52] studied the electrochemical activity of the Fe_3O_4-rGO composite with commercial AC electrode in which the battery-type electrode consisted of only 25% magnetite particles. As a consequence, a large irreversibility is observed in half-cell studies. The influence of Fe_3O_4-rGO on the AC concentration is also studied in the 1:1 to 1:5 ratio of Fe_3O_4-rGO to AC in the 1−4 V potential window; it is found that the 1:3 ratio exhibits high energy and power capability. As a result, the LIC is capable of delivering an energy density of ∼120 Wh kg^{-1} at lower rates. Interestingly, very decent cycling profile is also noted for 10 000 cycles with ∼84% retention. Obviously, this is one of the best results reported on conversion anode-based LICs. Kim et al.[53] made an attempt to increase the Fe_3O_4 loading to 65% in the Fe_3O_4-graphene (Fe_3O_4-G) composite using a microwave-assisted solvo-thermal approach without compromising the electrochemical performance (Figure 3). As expected, very stable half-cell profiles are noted for the Fe_3O_4-G composites electrochemically prelithiated before being paired with AC in the LIC. This assembly delivered a similar energy density (∼114 Wh kg^{-1}), but contrasting cycling profiles are noted. Increasing the Fe_3O_4 loading dramatically affected the cyclability; for example, only ∼70% of the initial density is retained after 2000 cycles. Fe_3O_4-filled N-doped carbon capsules (Fe_3O_4−NC) with hollow N-doped carbon capsules (HNC) have been reported with an extremely high energy density of ∼185 Wh kg^{-1} and good cycling stability.[54] Under very harsh conditions (28 kW kg^{-1}), this LIC maintains an energy density of ∼95 Wh kg^{-1}.

Similar to magnetite, hematite nanostructures have also been explored as negative electrodes in LIC configurations along with AC counter electrode.[56] Carbon coated α-Fe_2O_3 exhibited a high reversible capacity in the half-cell configuration, irrespective of the applied current rates, compared to the bare α-Fe_2O_3 electrode. This interesting assembly delivered a very high energy density of ∼90 Wh kg^{-1}. As expected, poor cycling profiles are noted in the LICs when hematite phases are employed as battery-type components. A citrate-mediated preparation of the hematite phase with a carbonaceous matrix is also reported as a promising negative electrode for LIC applications.[55] Hierarchical porous carbon (HPC) has been employed as a counter electrode and compared with commercial AC. Although deviating cycling profiles are

DOI: 10.1021/acs.jpclett.8b01386
J. Phys. Chem. Lett. 2018, 9, 3946−3958

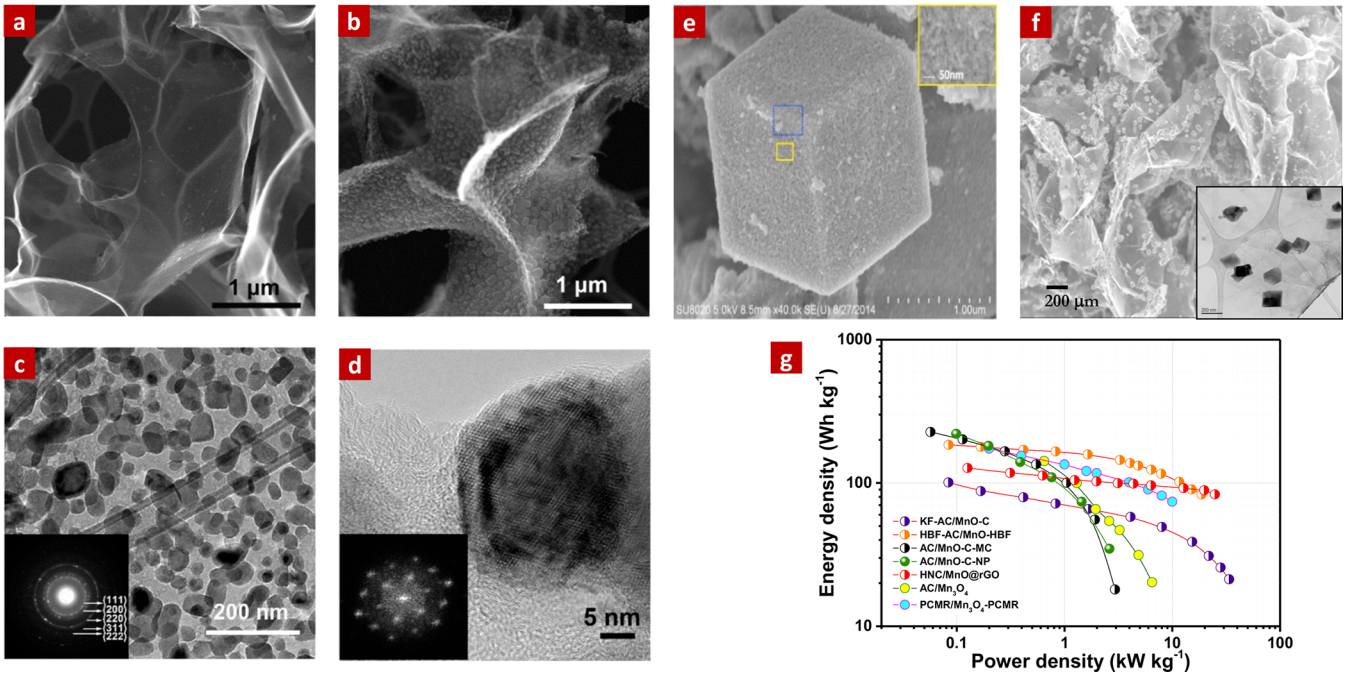

Figure 4. (a) SEM micrograph of 3D-HBF-AC. (b) Low-magnification SEM micrographs of 3D-MnO/HBF. (c) Bright-field TEM image of 3D-MnO/HBF. The inset displays the indexed SAED pattern. (d) HR-TEM image of a MnO nanocrystallite in 3D-MnO/HBF oriented in the [110] axis. The inset shows the associated fast Fourier transform. Reproduced with permission from ref 59. Copyright 2014, American Chemical Society. (e) SEM photograph of MnO produced by a PVA-assisted hydrothermal method with a cubic shape (MnO-C-MC). Reproduced with permission from ref 60. Copyright 2016, Elsevier. (f) Morphological features of Mn_3O_4-few layer graphene. Reproduced with permission from ref 65. Copyright 2016, The Royal Society of Chemistry. (g) Ragone plot of LICs based on various Mn-based active materials, including KF-AC/MnO-C,[64] AC/MnO-C-MC,[60] AC/MnO-C-NP,[61] HBF-AC/MnO-HBF,[59] HNC/MnO@rGO,[62] AC/Mn_3O_4,[65] and PCMR/Mn_3O_4–PCMR.[63]

noted for the citrate mediated Fe_2O_3@C in half-cell assemblies, they delivered an energy density of ~65 Wh kg^{-1} when paired with HPC. Karthikeyan et al.[57] and Zhao et al.[58] attempted the fabrication of hybrid capacitors without any prelithiation with F-doped Fe_2O_3 and MWCNT-Fe_2O_3 electrodes, respectively.

MnO is considered to be another promising conversion anode for LIBs; it has a theoretical capacity of ~756 mAh g^{-1}. The working potential for the redox reaction (MnO + 2Li + $2e^- \leftrightarrow Mn^0 + Li_2O$) is located at ~0.5 V vs Li, which eventually leads to the fabrication of high energy LICs.[11] Wang et al.[59] endeavored to use a composite of MnO with hemp bast fiber (HBF)-derived AC (HBF-AC) as a negative electrode and a HBF-AC with 3D architecture as a cathode. A reflux method is adopted to yield the MnO nanostructures. HBF-AC paired with MnO-HBF delivered a maximum energy density of ~184 Wh kg^{-1} in the 1–4 V potential range (Figure 4). Further, attempts have been made to use different anode to cathode mass loading ratios (1:1, 1:2, 1:4, 1:6, and 1:8) to yield high energy density; of these, superior performance is observed at the 1:2 ratio. As expected, narrowing down the testing potential range from 1–4 to 1–3.5 V results in a reduction in the energy density, but improves the retention characteristics. For instance, ~ 76% and ~81% of the initial density are recorded after 5000 cycles in the 1–4 and 1–3.5 V potential windows, respectively. Cao and co-workers[60,61] reported the possibility of exploring carbon-coated MnO mesocrystal cubes (MnO-C-MC) and nanoparticles (MnO-C-NP) for LIC applications. When the aforesaid MnO nanostructures are paired with AC counter electrode, energy densities of 227 and 220 Wh kg^{-1} are noted for MnO-C-MC and MnO-C-NP, respectively. In both cases, over 90% retention is observed during long-term cycling. Recently, Yang et al.[62] used ultrasmall MnO (5 nm) embedded rGO as a negative electrode with 3D hierarchical N-doped porous carbon (HNC) as the counter electrode. Prior to assembly formation, prelithiation is conducted for the battery-type conversion anode. The MnO@rGO/HNC-based LIC delivers an energy density as high as ~127 Wh kg^{-1} along with a high power capability. The decoration of ultrasmall Mn_3O_4 over porous carbon microrods (PCMR) has been suggested for battery-type component for the fabrication of LICs with PCMR as the counter electrode.[63] The Mn_3O_4–PCMR electrode is preactivated by conducting 10 galvanostatic cycles prior to assembling the LIC. Further, the influence of PCMR loading on Mn_3O_4–PCMR has been studied, and it is found that a 1:1 ratio leads to greater long-term stability unlike higher ratios. Although the battery-type component is not prelithiated, it delivered an energy density of ~174 Wh kg^{-1}. MnO anchored (24.9% loading) over kapok fiber-derived carbon as a negative electrode and KOH-activated kapok fiber-derived carbon (KF-AC) as a counter electrode is suggested for LICs.[64] Interestingly, the LIC is fabricated without prelithiation; instead, preactivation of the MnO-C component is carried out for several cycles before pairing it with KF-AC. Further, attempts have been made to alter MnO-C with respect to the EDLC component loading (from 1:1 to 1:4) to achieve higher values of energy. A 1:2 loading is found to yield high energy density (~100 Wh kg^{-1}) and power capability. Unfortunately, fading is noted in the cycling profiles. Recently, Ulaganathan et al.[65] reported the possibility of using Mn_3O_4-few layer graphene as a battery-type component with commercial AC as the counter electrode. Apparently, the composite undergoes perfect intercalation and conversion due

DOI: 10.1021/acs.jpclett.8b01386
J. Phys. Chem. Lett. 2018, 9, 3946–3958

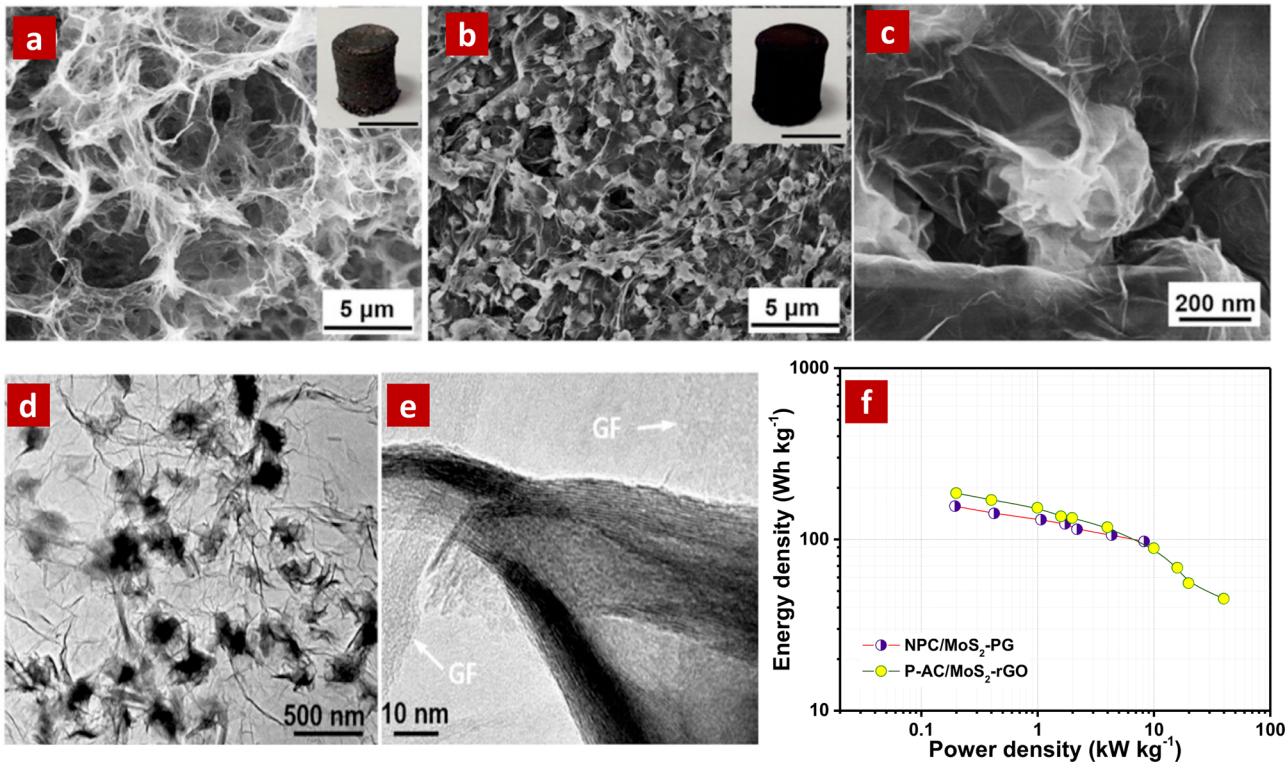

Figure 5. (a) SEM image of the NPC sample (inset: photograph of the NPC bulk sample, scale bar: 1 cm). (b) SEM image of the MoS_2−PG composite (inset: photograph of the MoS_2−PG bulk sample, scale bar: 1 cm). (c) SEM image of the MoS_2−PG composite at a high magnification. (d,e) TEM images of the MoS_2−PG composite at different magnifications. Reproduced with permission from ref 71. Copyright 2016, American Chemical Society. (f) Ragone plot of the LICs based on various Mo-based active materials, including NPC/MoS_2−PG[71] and P-AC/MoS_2-rGO.[72]

to the presence of a few layers of graphene and Mn_3O_4, respectively. Although Mn_3O_4 undergoes a conversion reaction, the oxidation of the native phase (Mn_3O_4) is not possible during the charge process. Therefore, the conversion of MnO_x to the metallic phase (Mn^0) and its reversibility is only possible as described above and elsewhere.[66] An electrochemically lithiated phase was used as the battery-type component with AC, but delivered an energy density of ∼142 Wh kg^{-1} with a decent cycling profile of 9000 cycles.

Molybdenum disulfide, MoS_2, is one of the most extensively studied electrodes for LIB applications.[67,68] MoS_2 has been investigated as an insertion-type cathode owing to the weak van der Waals bonds between the S−Mo−S layers. This weak interaction eventually suppresses volume variations engendered during Li-insertion/extraction (Li_xMoS_2). Unfortunately, its redox potential is too low for cathode applications and too high for anode applications.[67] The emergence of high voltage cathodes, such as $LiCoO_2$ and $LiMn_2O_4$, gained worldwide attention, and their commercialization put an end card to the research on MoS_2-based cathodes.[69] After the discovery of sustained Li-storage via a conversion pathway using nanostructured materials,[70] research activity on MoS_2 gained much ground; MoS_2 exhibits ($MoS_2 + 4Li^+ + 4e^- \leftrightarrow Mo^0 + 2Li_2S$) a high theoretical capacity (∼669 mAh g^{-1}) and high power capability. Although there is no possibility for the commercialization of conversion-type electrodes, academic interest cannot be discounted.[11,16,66] In this regard, Zhang et al.[71] exploited the possibility of using MoS_2-decorated 3D porous graphene nanosheets (MoS_2−PG) as negative electrode for the fabrication of LICs with nitrogen-doped porous carbon (NPC). A reversible capacity of ∼1022 mAh g^{-1} is noted in the case of MoS_2−PG during the preliminary Li-storage studies in a half-cell assembly. As expected, severe fading is observed in the capacity profiles of bare MoS_2 as compared to those of MoS_2−PG. The NPC/MoS_2−PG-based LIC registered a maximum energy density of ∼156 Wh kg^{-1}, which is much higher than that of a commercial AC-based system (∼102 Wh kg^{-1}, AC/MoS_2−PG). Similarly, Wang et al.[72] engineered a MoS_2-graphene composite as a battery-type component for LIC applications with polyaniline-derived carbon activated with KOH as the counter electrode (P-AC). Very impressive cycling profiles are registered for such MoS_2-rGO composite, irrespective of the half-cell assembly (>300) or the LIC assembly (>10 000), owing to the hydrothermal approach they adopted. Eventually, this system delivers a maximum energy density of ∼188 Wh kg^{-1} up to 4 V (Figure 5).

$MnFe_2O_4$ (Jacobsite) is a low-cost and stable magnetic spinel ferrite material; it has been explored as a conversion-type anode for Li-ion power packs with a maximum possible capacity of ∼930 mAh g^{-1} for an eight electron reaction. The Li-storage mechanism of this interesting material can be described as $MnFe_2O_4 + 8Li^+ + 8e^- \rightarrow Mn^0 + 2Fe^0 + 4Li_2O$. Upon charging and subsequent cycling, the native spinel will not be reformed; it appears to be a composite of individual metal oxides (MnO and Fe_2O_3) embedded in the amorphous Li_2O matrix. Therefore, the reaction mechanism can be described as $Mn^0 + Li_2O \leftrightarrow MnO + 2Li^+ + 2e^-$ and $Fe^0 + 3Li_2O \leftrightarrow Fe_2O_3 + 6Li^+ + 6e^-$. In this regard, Lee et al.[73] explored the possibility of using $MnFe_2O_4$ nanocubes embedded in a carbon matrix ($MnFe_2O_4$−C) as a possible battery-type component in LIC assemblies with three different

DOI: 10.1021/acs.jpclett.8b01386
J. Phys. Chem. Lett. 2018, 9, 3946−3958

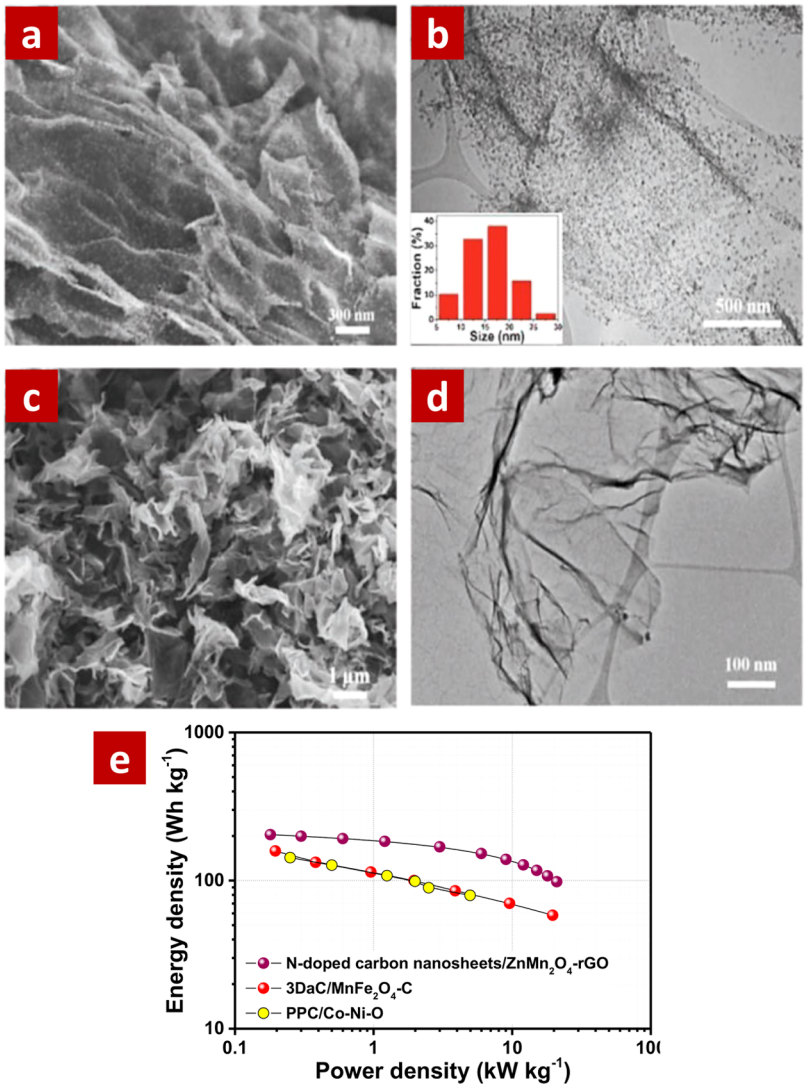

Figure 6. (a,b) SEM and TEM images of $ZnMn_2O_4$-rGO, (c,d) SEM and TEM images of N-doped carbon nanosheets. Reproduced with permission from ref 76. Copyright 2017 John Wiley and Sons. (e) Ragone plot of LICs based on 3 DaC/$MnFe_2O_4$−C,[73] PPC/Co−Ni−O,[74] and $ZnMn_2O_4$-rGO/N-doped carbon nanosheets.[76]

carbonaceous materials: rGO, 3D amorphous carbon (3DaC), and graphitic activated carbon. Among these, 3DaC exhibited the best electrochemical characteristics in both half-cell and LIC assemblies. A prelithiated $MnFe_2O_4$−C/3 DaC-based LIC registered a maximum energy density of ∼157 Wh kg^{-1}. Even in extremely harsh conditions (20 kW kg^{-1}), the LIC is capable of delivering ∼58 Wh kg^{-1} (Figure 6). Additionally, a very good cyclability is also noted with this configuration.

Liu et al.[74] suggested the possibility of using Co−Ni−O microflowers prepared via a simple coprecipitation route as a possible battery-type component with polyaniline-derived porous carbon (PPC) as a counter electrode. The researchers explored various mass ratios between the metal oxide and PPC to achieve high energy configurations. A 1:2 ratio of metal oxide to PPC is found to be superior in terms of its Li-ion kinetics. Prior to LIC fabrication, the metal oxide is electrochemically prelithiated and coupled with PPC. The LIC is capable of delivering an energy density of ∼143 Wh kg^{-1} with extremely long cyclability of 15 000 cycles with ∼78% retention. It is worth mentioning that the Ni−Co−O ternary oxide with a presodiated phase has also been successfully adopted for Na-ion capacitors along with AC counter electrodes to achieve an energy density of over 120 Wh kg^{-1}.[75]

Li et al.[76] explored the usage of $ZnMn_2O_4$ embedded in a 2D rGO matrix as a battery-type component for LIC applications along with N-doped carbon sheets. In contrast to the aforementioned ternary oxides, $ZnMn_2O_4$ undergoes both conversion and alloying reactions. More clearly, Zn undergoes both alloying and conversion according to the testing potential window used. For example, the reaction mechanism during discharge process is $ZnMn_2O_4 + 8Li^+ + 8e^- \rightarrow Zn^0 + 2Mn^0 + 4Li_2O$ and subsequently Zn will form an alloy with Li according to $Zn^0 + Li^+ + e^- \leftrightarrow LiZn$. Upon charging, the LiZn alloy is decomposed and oxidized to the native oxide (ZnO) as follows: $LiZn \leftrightarrow Zn^0 + Li^+ + e^- \leftrightarrow ZnO$; on the other hand, metallic Mn^0 is oxidized to Mn^{2+} ($Mn^0 \leftrightarrow MnO$) (Scheme 2C). Nevertheless, the electrochemical activities of individual MnO-rGO and ZnO-rGO composites are compared with that of a $ZnMn_2O_4$-rGO composite in a half-cell assembly. The $ZnMn_2O_4$-rGO composite exhibited superior properties than the individual

DOI: 10.1021/acs.jpclett.8b01386
J. Phys. Chem. Lett. 2018, 9, 3946−3958

oxides, suggesting that ternary oxides are promising battery-type components for LICs. The $ZnMn_2O_4$-rGO composite is prelithiated by a spontaneous lithiation process and coupled with N-doped carbon sheets. The LIC delivered a maximum energy density of ∼203 Wh kg^{-1} with a decent cycling profile of 3000 galvanic cycles with ∼70% retention.

Limited improvements in the anion adsorption/desorption properties and energy are noted while modifying the high surface area carbonaceous counterparts. However, the improvement is not sufficient to fabricate high energy LIC assemblies. The real enhancement lies in the development of battery-type components. Spinel $Li_4Ti_5O_{12}$ is proposed as a prospective intercalation-type anode for LIC perspective and used in commercial configurations. Unfortunately, their high insertion potential (>1 V) and limited capacity of insertion-type electrodes compared to graphitic anodes dilutes the net energy density of LICs based on such electrodes. Therefore, the utilization of conversion- and alloy-type materials as battery-type components is deemed an efficient approach to achieve high energy densities, taking into account their high reversible capacity, lower working potential than insertion-type electrodes (except graphite and HC), and high power capability. The testing window is one of the most important parameters to assess, apart from the mass balance between the electrodes, to achieve high energy density and cyclability. In particular, alloy-type materials exhibit comparatively lower working potentials (vs Li); hence, there is a possible risk of Li-platting during high current operations, which is similar to the conditions faced by graphitic anodes. On the other hand, conversion anodes exhibit slightly higher redox potentials than alloy-type anodes, but marginally lower than those of insertion-type anodes. Thus, more research is needed on alloy-type anodes, in particular, on Group IV elements, such as Sb, Sn, and Ge and Si-based derivatives. Overall, both conversion and alloy-type materials display higher energy densities than insertion-type materials (including graphite and HC). This can be clearly seen from the various configurations developed with a variety of materials.[11] One of the major issues is the consistency in the energy density, which is severely affected by many factors, such as the testing window, counter electrode, and redox potential. Another important issue is the huge ICL observed in the first cycle for such high capacity anodes. Usually, graphite or HC is lithiated using tailor-made procedures, such as spontaneous lithiation, chemical lithiation, and electrochemical lithiation, which is sufficient to form a stable SEI layer.[1] However, the formation of a stable SEI and its composition are completely different in conversion- and alloy-type anodes when compared to carbonaceous anodes.[77] Therefore, fewer initial cycles are required to form stable SEI layer over active materials. As a result, fewer cycles are required with metallic Li to ensure the complete elimination of ICL before fabricating the LIC assembly. This is the only time-consuming process compared to carbonaceous insertion hosts. Although the usage of stabilized lithium metal powder is possible, it is expensive, and controlling the amount of loading is also difficult.[1,78,79] If an excess amount of metallic Li is present, it may trigger unwanted side reactions with electrolyte counterparts. The time-consuming prelithiation step is one of the major differences between the conversion- and alloy-type anodes and their carbonaceous counterparts.[1] As described earlier, high-capacity anodes experience extremely large volume variations, especially alloy-type anodes, but this issue can be efficiently tackled by fabricating hollow-structured materials or composites with active and inactive matrices, as stated. The evolution of such methodologies indicates the maturity of the research domain on conversion and alloy-type negative electrodes. Despite facing the serious concern of limited cyclability compared to the LIC based in insertion-type materials, conversion- and alloy-type materials have a bright future in LIC applications for the development of high energy and high power devices with long life spans. We anticipate that the research activity/direction on LIC must be focused to address the issue of limited cyclability of such fascinating active materials, besides the exploration of new materials. Moreover, this concept has already been successfully implemented in Na-ion capacitor analogues to achieve higher values than those possible with the existing intercalation-based configurations.[75,80]

Fixing the testing window is another crucial parameter for achieving higher values and subsequently commercializing such active materials. However, one should be careful while fixing the testing window; otherwise, it may lead to Li-platting and subsequently to explosions because LICs are usually tested at higher rates than LIBs. Of course, the redox potential of the battery-type active material is one of the crucial factors to achieve high power and energy. Nevertheless, the influence of the carbonaceous counter electrode cannot be ruled out; for example, the usage of a very high surface area AC triggers the decomposition of the electrolyte well before the actual potential is reached. Therefore, the usage of very large surface area is not advised during LIC assembly. While handling such extremely large surface area carbonaceous materials, researchers face the problem of adhesion with the current collector. Therefore, an optimum surface area is suggested for achieving high performance LICs with good durability. This is one of the major reasons behind the difficulty in comparing the obtained results of alloying and conversion anodes all together. Many reports are available on biomass-derived ACs, some of them enriched with N doping and a few of them with rGO. Each and every carbonaceous material has its own features, surface area, porosity, and capacity of promoting electrochemical activity, similar to battery-type electrodes.[81,82] Although the present report is focused on the usage of alloy and conversion-type anodes rather than the traditional intercalation-type materials in LICs, it is well-known that alloy and conversion-type materials are active in the nanosized range only. Their electrochemical activity in the bulk form is very poor, unlike that of intercalation-type metal oxides and phosphates.[16] From the material perspective, unlike the limited options available for transition metal-based insertion hosts, numerous other metal oxides, sulfides, hydroxides, and carbonates could be explored as electrodes for building next-generation LICs with high energy and high power capability. Exploring the active materials in morphological features is also certainly possible.

AUTHOR INFORMATION

Corresponding Authors

*E-mail: aravind_van@yahoo.com (V.A.).
*E-mail: leeys@chonnam.ac.kr (Y.-S.L.).

ORCID

Vanchiappan Aravindan: 0000-0003-1357-7717
Yun-Sung Lee: 0000-0002-6676-2871

Notes

The authors declare no competing financial interest.

DOI: 10.1021/acs.jpclett.8b01386
J. Phys. Chem. Lett. 2018, 9, 3946−3958

Biographies

Vanchiappan Aravindan is currently working as a Ramanujan Faculty in the Department of Chemistry, Indian Institute of Sciecne Education and Research (IISER), Tirupati, India. He received his Ph.D. in 2009 at Gandhigram Rural University, Gandhigram, India. He then became a Post Doctoral Fellow at Chonnam National University, Gwang-ju in Korea, with Prof. Yun-Sung Lee. Later, he joined (2010−2017) as a Senior Scientist at the Energy Research Institute @ NTU (ERI@N), Nanyang Technological University, Singapore. His research interests include the development of high performance electrodes and electrolytes for Li-ion chemistry and beyond.

Yun-Sung Lee is currently working as Full Professor at Chonnam National University, Gwang-ju, in Korea. He received his M.S. from Chonbuk National University in 1998 and his research work was carried out under the guidance of Prof. Kee-Suk Nahm. He received a Ph.D in 2001 in Applied Chemistry from Saga University in Japan under the direction of Prof. Masaki Yoshio. In 2001 he joined as a Post-Doctoral Fellow and Doctoral Researcher with Professor Yuichi Sato, at Kanagawa University in Japan. In 2003 he joined Chonnam National University as an Assistant Professor. His research interests are in the fields of Li-ion battery, electrode materials, and hybrid capacitor systems.

■ ACKNOWLEDGMENTS

This study was supported by the National Research Foundation of Korea (NRF) grant funded by the Korea government (Ministry of Science, ICT & Future Planning) (No. 2016R1A4A1012224). V.A. acknowledges financial support from the Science & Engineering Research Board (SERB), a statutory body of the Department of Science & Technology, Govt. of India, through the Ramanujan Fellowship (SB/S2/RJN-088/2016).

■ REFERENCES

(1) Aravindan, V.; Lee, Y.-S.; Madhavi, S. Best Practices for Mitigating Irreversible Capacity Loss of Negative Electrodes in Li-Ion Batteries. *Adv. Energy Mater.* **2017**, *7*, 1602607.
(2) Aravindan, V.; Gnanaraj, J.; Lee, Y.-S.; Madhavi, S. Insertion-Type Electrodes for Nonaqueous Li-Ion Capacitors. *Chem. Rev.* **2014**, *114*, 11619−11635.
(3) Amatucci, G. G.; Badway, F.; Du Pasquier, A.; Zheng, T. An Asymmetric Hybrid Nonaqueous Energy Storage Cell. *J. Electrochem. Soc.* **2001**, *148*, A930−A939.
(4) Plitz, I.; DuPasquier, A.; Badway, F.; Gural, J.; Pereira, N.; Gmitter, A.; Amatucci, G. G. The design of alternative nonaqueous high power chemistries. *Appl. Phys. A: Mater. Sci. Process.* **2006**, *82*, 615−626.
(5) Pasquier, A. D.; Plitz, I.; Gural, J.; Badway, F.; Amatucci, G. G. Power-ion battery: Bridging the gap between Li-ion and supercapacitor chemistries. *J. Power Sources* **2004**, *136*, 160−170.
(6) Naoi, K.; Naoi, W.; Aoyagi, S.; Miyamoto, J.-i.; Kamino, T. New Generation "Nanohybrid Supercapacitor. *Acc. Chem. Res.* **2013**, *46*, 1075−1083.
(7) Naoi, K.; Ishimoto, S.; Miyamoto, J.-i.; Naoi, W. Second generation 'nanohybrid supercapacitor': Evolution of capacitive energy storage devices. *Energy Environ. Sci.* **2012**, *5*, 9363−9373.
(8) Naoi, K.; Nagano, Y. Li-Ion-Based Hybrid Supercapacitors in Organic Medium. In *Supercapacitors*; Wiley-VCH Verlag GmbH & Co. KGaA: Weinheim, Germany, 2013; pp 239−256.
(9) Khomenko, V.; Raymundo-Piñero, E.; Béguin, F. High-energy density graphite/AC capacitor in organic electrolyte. *J. Power Sources* **2008**, *177*, 643−651.
(10) Sivakkumar, S. R.; Pandolfo, A. G. Evaluation of lithium-ion capacitors assembled with pre-lithiated graphite anode and activated carbon cathode. *Electrochim. Acta* **2012**, *65*, 280−287.
(11) Aravindan, V.; Lee, Y.-S.; Madhavi, S. Research Progress on Negative Electrodes for Practical Li-Ion Batteries: Beyond Carbonaceous Anodes. *Adv. Energy Mater.* **2015**, *5*, 1402225.
(12) Aravindan, V.; Sundaramurthy, J.; Suresh Kumar, P.; Lee, Y. S.; Ramakrishna, S.; Madhavi, S. Electrospun nanofibers: A prospective electro-active material for constructing high performance Li-ion batteries. *Chem. Commun.* **2015**, *51*, 2225−2234.
(13) Aravindan, V.; Lee, Y.-S.; Yazami, R.; Madhavi, S. TiO_2 polymorphs in 'rocking-chair' Li-ion batteries. *Mater. Today* **2015**, *18*, 345−351.
(14) Kim, J.-H.; Kim, J.-S.; Lim, Y.-G.; Lee, J.-G.; Kim, Y.-J. Effect of carbon types on the electrochemical properties of negative electrodes for Li-ion capacitors. *J. Power Sources* **2011**, *196*, 10490−10495.
(15) Satish, R.; Aravindan, V.; Ling, W. C.; Goodenough, J. B.; Madhavi, S. Carbon-Coated $Li_3Nd_3W_2O_{12}$: A High Power and Low-Voltage Insertion Anode with Exceptional Cycleability for Li-Ion Batteries. *Adv. Energy Mater.* **2014**, *4*, 1301715.
(16) Reddy, M. V.; Subba Rao, G. V.; Chowdari, B. V. R. Metal Oxides and Oxysalts as Anode Materials for Li Ion Batteries. *Chem. Rev.* **2013**, *113*, 5364−5457.
(17) Sennu, P.; Aravindan, V.; Ganesan, M.; Lee, Y. G.; Lee, Y. S. Biomass-Derived Electrode for Next Generation Lithium-Ion Capacitors. *ChemSusChem* **2016**, *9*, 849−854.
(18) Jayaraman, S.; Jain, A.; Ulaganathan, M.; Edison, E.; Srinivasan, M.; Balasubramanian, R.; Aravindan, V.; Madhavi, S. Li-ion vs. Na-ion capacitors: A performance evaluation with coconut shell derived mesoporous carbon and natural plant based hard carbon. *Chem. Eng. J.* **2017**, *316*, 506−513.
(19) Chou, C.-Y.; Kim, H.; Hwang, G. S. A Comparative First-Principles Study of the Structure, Energetics, and Properties of Li−M (M = Si, Ge, Sn) Alloys. *J. Phys. Chem. C* **2011**, *115*, 20018−20026.
(20) Aravindan, V.; Sundaramurthy, J.; Suresh Kumar, P.; Lee, Y.-S.; Ramakrishna, S.; Madhavi, S. Electrospun nanofibers: A prospective electro-active material for constructing high performance Li-ion batteries. *Chem. Commun.* **2015**, *51*, 2225−2234.
(21) Wu, H.; Cui, Y. Designing nanostructured Si anodes for high energy lithium ion batteries. *Nano Today* **2012**, *7*, 414−429.

DOI: 10.1021/acs.jpclett.8b01386
J. Phys. Chem. Lett. 2018, 9, 3946−3958

(22) Park, C.-M.; Kim, J.-H.; Kim, H.; Sohn, H.-J. Li-alloy based anode materials for Li secondary batteries. *Chem. Soc. Rev.* **2010**, *39*, 3115−3141.
(23) Huggins, R. A. Alternative materials for negative electrodes in lithium systems. *Solid State Ionics* **2002**, *152−153*, 61−68.
(24) Chen, Z.; Chevrier, V.; Christensen, L.; Dahn, J. R. Design of amorphous alloy electrodes for Li-ion batteries a big challenge. *Electrochem. Solid-State Lett.* **2004**, *7*, A310−A314.
(25) Beaulieu, L. Y.; Hewitt, K. C.; Turner, R. L.; Bonakdarpour, A.; Abdo, A. A.; Christensen, L.; Eberman, K. W.; Krause, L. J.; Dahn, J. R. The Electrochemical Reaction of Li with Amorphous Si-Sn Alloys. *J. Electrochem. Soc.* **2003**, *150*, A149−A156.
(26) Chan, C. K.; Peng, H.; Liu, G.; McIlwrath, K.; Zhang, X. F.; Huggins, R. A.; Cui, Y. High-performance lithium battery anodes using silicon nanowires. *Nat. Nanotechnol.* **2008**, *3*, 31−35.
(27) Wen, C. J.; Huggins, R. A. Chemical diffusion in intermediate phases in the lithium-silicon system. *J. Solid State Chem.* **1981**, *37*, 271−278.
(28) Li, H.; Shi, L.; Lu, W.; Huang, X.; Chen, L. Studies on Capacity Loss and Capacity Fading of Nanosized SnSb Alloy Anode for Li-Ion Batteries. *J. Electrochem. Soc.* **2001**, *148*, A915−A922.
(29) Choi, N.-S.; Yao, Y.; Cui, Y.; Cho, J. One dimensional Si/Sn - based nanowires and nanotubes for lithium-ion energy storage materials. *J. Mater. Chem.* **2011**, *21*, 9825−9840.
(30) Liu, N.; Lu, Z.; Zhao, J.; McDowell, M. T.; Lee, H.-W.; Zhao, W.; Cui, Y. A pomegranate-inspired nanoscale design for large-volume-change lithium battery anodes. *Nat. Nanotechnol.* **2014**, *9*, 187−192.
(31) Saito, M.; Takahashi, K.; Ueno, K.; Seki, S. Electrochemical Charge/Discharge Properties of Li Pre-doped Si Nanoparticles for Use in Hybrid Capacitor Systems. *J. Electrochem. Soc.* **2016**, *163*, A3140−A3145.
(32) Liu, X.; Jung, H.-G.; Kim, S.-O.; Choi, H.-S.; Lee, S.; Moon, J. H.; Lee, J. K. Silicon/copper dome-patterned electrodes for high-performance hybrid supercapacitors. *Sci. Rep.* **2013**, *3*, 3183.
(33) Yi, R.; Chen, S.; Song, J.; Gordin, M. L.; Manivannan, A.; Wang, D. High-Performance Hybrid Supercapacitor Enabled by a High-Rate Si-based Anode. *Adv. Funct. Mater.* **2014**, *24*, 7433−7439.
(34) Li, B.; Dai, F.; Xiao, Q.; Yang, L.; Shen, J.; Zhang, C.; Cai, M. Nitrogen-doped activated carbon for a high energy hybrid supercapacitor. *Energy Environ. Sci.* **2016**, *9*, 102−106.
(35) Fridman, K.; Sharabi, R.; Elazari, R.; Gershinsky, G.; Markevich, E.; Salitra, G.; Aurbach, D.; Garsuch, A.; Lampert, J. A new advanced lithium ion battery: Combination of high performance amorphous columnar silicon thin film anode, 5 V $LiNi_{0.5}Mn_{1.5}O_4$ spinel cathode and fluoroethylene carbonate-based electrolyte solution. *Electrochem. Commun.* **2013**, *33*, 31−34.
(36) Fridman, K.; Sharabi, R.; Markevich, E.; Elazari, R.; Salitra, G.; Gershinsky, G.; Aurbach, D.; Lampert, J.; Schulz-Dobrick, M. An Advanced Lithium Ion Battery Based on Amorphous Silicon Film Anode and Integrated $xLi_2MnO_3.(1-x)LiNi_yMn_zCo_{1-y-z}O_2$ Cathode. *ECS Electrochem. Lett.* **2013**, *2*, A84−A87.
(37) Markevich, E.; Fridman, K.; Sharabi, R.; Elazari, R.; Salitra, G.; Gottlieb, H. E.; Gershinsky, G.; Garsuch, A.; Semrau, G.; Schmidt, M. A.; et al. Amorphous Columnar Silicon Anodes for Advanced High Voltage Lithium Ion Full Cells: Dominant Factors Governing Cycling Performance. *J. Electrochem. Soc.* **2013**, *160*, A1824−A1833.
(38) Li, B.; Dai, F.; Xiao, Q.; Yang, L.; Shen, J.; Zhang, C.; Cai, M. Activated Carbon from Biomass Transfer for High-Energy Density Lithium-Ion Supercapacitors. *Adv. Energy Mater.* **2016**, *6*, 1600802.
(39) Halim, M.; Liu, G.; Ardhi, R. E. A.; Hudaya, C.; Wijaya, O.; Lee, S.-H.; Kim, A. Y.; Lee, J. K. Pseudocapacitive Characteristics of Low-Carbon Silicon Oxycarbide for Lithium-Ion Capacitors. *ACS Appl. Mater. Interfaces* **2017**, *9*, 20566−20576.
(40) http://www.sony.net/SonyInfo/News/Press/200502/05-006E/ (Accessed on May 19, 2018).
(41) Aravindan, V.; Gnanaraj, J.; Lee, Y.-S.; Madhavi, S. LiMnPO4 - A next generation cathode material for lithium-ion batteries. *J. Mater. Chem. A* **2013**, *1*, 3518−3539.
(42) Todd, A. D. W.; Ferguson, P. P.; Fleischauer, M. D.; Dahn, J. R. Tin-based materials as negative electrodes for Li-ion batteries: Combinatorial approaches and mechanical methods. *Int. J. Energy Res.* **2010**, *34*, 535−555.
(43) Sun, F.; Gao, J.; Zhu, Y.; Pi, X.; Wang, L.; Liu, X.; Qin, Y. A high performance lithium ion capacitor achieved by the integration of a Sn-C anode and a biomass-derived microporous activated carbon cathode. *Sci. Rep.* **2017**, *7*, 40990.
(44) Won, J. H.; Jeong, H. M.; Kang, J. K. Synthesis of Nitrogen-Rich Nanotubes with Internal Compartments having Open Mesoporous Channels and Utilization to Hybrid Full-Cell Capacitors Enabling High Energy and Power Densities over Robust Cycle Life. *Adv. Energy Mater.* **2017**, *7*, 1601355.
(45) Sennu, P.; Aravindan, V.; Lee, Y.-S. Marine algae inspired pre-treated SnO_2 nanorods bundle as negative electrode for Li-ion capacitor and battery: An approach beyond intercalation. *Chem. Eng. J.* **2017**, *324*, 26−34.
(46) Qu, W.-H.; Han, F.; Lu, A.-H.; Xing, C.; Qiao, M.; Li, W.-C. Combination of a SnO_2-C hybrid anode and a tubular mesoporous carbon cathode in a high energy density non-aqueous lithium ion capacitor: preparation and characterisation. *J. Mater. Chem. A* **2014**, *2*, 6549−6557.
(47) Hsieh, C.-L.; Tsai, D.-S.; Chiang, W.-W.; Liu, Y.-H. A composite electrode of tin dioxide and carbon nanotubes and its role as negative electrode in lithium ion hybrid capacitor. *Electrochim. Acta* **2016**, *209*, 332−340.
(48) Ajuria, J.; Arnaiz, M.; Botas, C.; Carriazo, D.; Mysyk, R.; Rojo, T.; Talyzin, A. V.; Goikolea, E. Graphene-based lithium ion capacitor with high gravimetric energy and power densities. *J. Power Sources* **2017**, *363*, 422−427.
(49) Lukatskaya, M. R.; Dunn, B.; Gogotsi, Y. Multidimensional materials and device architectures for future hybrid energy storage. *Nat. Commun.* **2016**, *7*, 12647.
(50) Luo, J.; Zhang, W.; Yuan, H.; Jin, C.; Zhang, L.; Huang, H.; Liang, C.; Xia, Y.; Zhang, J.; Gan, Y.; Tao, X. Pillared Structure Design of MXene with Ultralarge Interlayer Spacing for High-Performance Lithium-Ion Capacitors. *ACS Nano* **2017**, *11*, 2459−2469.
(51) Zhang, F.; Zhang, T.; Yang, X.; Zhang, L.; Leng, K.; Huang, Y.; Chen, Y. A high-performance supercapacitor-battery hybrid energy storage device based on graphene-enhanced electrode materials with ultrahigh energy density. *Energy Environ. Sci.* **2013**, *6*, 1623−1632.
(52) Zhang, S.; Li, C.; Zhang, X.; Sun, X.; Wang, K.; Ma, Y. High Performance Lithium-Ion Hybrid Capacitors Employing Fe_3O_4−Graphene Composite Anode and Activated Carbon Cathode. *ACS Appl. Mater. Interfaces* **2017**, *9*, 17136−17144.
(53) Kim, H.-K.; Aravindan, V.; Roh, M. H.-K.; Lee, K.; Jung, M.-H.; Madhavi, S.; Roh, K. C.; Kim, K.-B. Exploring High-Energy Li-i(r)on Batteries and Capacitors with Conversion-Type Fe_3O_4-rGO as the Negative Electrode. *ChemElectroChem* **2017**, *4*, 2626−2633.
(54) An, C.; Liu, X.; Gao, Z.; Ding, Y. Filling and unfilling carbon capsules with transition metal oxide nanoparticles for Li-ion hybrid supercapacitors: towards hundred grade energy density. *Sci. China Mater.* **2017**, *60*, 217−227.
(55) Yu, X.; Deng, J.; Zhan, C.; Lv, R.; Huang, Z.-H.; Kang, F. A high-power lithium-ion hybrid electrochemical capacitor based on citrate-derived electrodes. *Electrochim. Acta* **2017**, *228*, 76−81.
(56) Brandt, A.; Balducci, A. A study about the use of carbon coated iron oxide-based electrodes in lithium-ion capacitors. *Electrochim. Acta* **2013**, *108*, 219−225.
(57) Karthikeyan, K.; Amaresh, S.; Lee, S. N.; Aravindan, V.; Lee, Y. S. Fluorine-Doped Fe2O3 as High Energy Density Electroactive Material for Hybrid Supercapacitor Applications. *Chem. - Asian J.* **2014**, *9*, 852−857.
(58) Zhao, X.; Johnston, C.; Grant, P. S. A novel hybrid supercapacitor with a carbon nanotube cathode and an iron oxide/carbon nanotube composite anode. *J. Mater. Chem.* **2009**, *19*, 8755−8760.

DOI: 10.1021/acs.jpclett.8b01386
J. Phys. Chem. Lett. 2018, 9, 3946−3958

(59) Wang, H.; Xu, Z.; Li, Z.; Cui, K.; Ding, J.; Kohandehghan, A.; Tan, X.; Zahiri, B.; Olsen, B. C.; Holt, C. M. B.; et al. Hybrid Device Employing Three-Dimensional Arrays of MnO in Carbon Nanosheets Bridges Battery−Supercapacitor Divide. *Nano Lett.* **2014**, *14*, 1987−1994.
(60) Liu, C.; Zhang, C.; Song, H.; Zhang, C.; Liu, Y.; Nan, X.; Cao, G. Mesocrystal MnO cubes as anode for Li-ion capacitors. *Nano Energy* **2016**, *22*, 290−300.
(61) Liu, C.; Zhang, C.; Song, H.; Nan, X.; Fu, H.; Cao, G. MnO nanoparticles with cationic vacancies and discrepant crystallinity dispersed into porous carbon for Li-ion capacitors. *J. Mater. Chem. A* **2016**, *4*, 3362−3370.
(62) Yang, M.; Zhong, Y.; Ren, J.; Zhou, X.; Wei, J.; Zhou, Z. Fabrication of High-Power Li-Ion Hybrid Supercapacitors by Enhancing the Exterior Surface Charge Storage. *Adv. Energy Mater.* **2015**, *5*, 1500550.
(63) Wang, R.; Liu, P.; Lang, J.; Zhang, L.; Yan, X. Coupling effect between ultra-small Mn_3O_4 nanoparticles and porous carbon microrods for hybrid supercapacitors. *Energy Storage Mater.* **2017**, *6*, 53−60.
(64) Zhao, Y.; Cui, Y.; Shi, J.; Liu, W.; Shi, Z.; Chen, S.; Wang, X.; Wang, H. Two-dimensional biomass-derived carbon nanosheets and MnO/carbon electrodes for high-performance Li-ion capacitors. *J. Mater. Chem. A* **2017**, *5*, 15243−15252.
(65) Ulaganathan, M.; Aravindan, V.; Ling, W. C.; Yan, Q.; Madhavi, S. High energy Li-ion capacitors with conversion type Mn_3O_4 particulates anchored to few layer graphene as the negative electrode. *J. Mater. Chem. A* **2016**, *4*, 15134−15139.
(66) Fang, X.; Lu, X.; Guo, X.; Mao, Y.; Hu, Y.-S.; Wang, J.; Wang, Z.; Wu, F.; Liu, H.; Chen, L. Electrode reactions of manganese oxides for secondary lithium batteries. *Electrochem. Commun.* **2010**, *12*, 1520−1523.
(67) Stephenson, T.; Li, Z.; Olsen, B.; Mitlin, D. Lithium ion battery applications of molybdenum disulfide (MoS_2) nanocomposites. *Energy Environ. Sci.* **2014**, *7*, 209−231.
(68) Whittingham, M. S. Lithium Batteries and Cathode Materials. *Chem. Rev.* **2004**, *104*, 4271−4302.
(69) Goodenough, J. B.; Park, K.-S. The Li-Ion Rechargeable Battery: A Perspective. *J. Am. Chem. Soc.* **2013**, *135*, 1167−1176.
(70) Poizot, P.; Laruelle, S.; Grugeon, S.; Dupont, L.; Tarascon, J. M. Nano-sized transition-metal oxides as negative-electrode materials for lithium-ion batteries. *Nature* **2000**, *407*, 496−499.
(71) Zhang, F.; Tang, Y.; Liu, H.; Ji, H.; Jiang, C.; Zhang, J.; Zhang, X.; Lee, C.-S. Uniform Incorporation of Flocculent Molybdenum Disulfide Nanostructure into Three-Dimensional Porous Graphene as an Anode for High-Performance Lithium Ion Batteries and Hybrid Supercapacitors. *ACS Appl. Mater. Interfaces* **2016**, *8*, 4691−4699.
(72) Wang, R.; Wang, S.; Jin, D.; Zhang, Y.; Cai, Y.; Ma, J.; Zhang, L. Engineering layer structure of MoS_2-graphene composites with robust and fast lithium storage for high-performance Li-ion capacitors. *Energy Storage Mater.* **2017**, *9*, 195−205.
(73) Lee, W. S. V.; Peng, E.; Li, M.; Huang, X.; Xue, J. M. Rational Design of Stable 4 V Lithium Ion Capacitor. *Nano Energy* **2016**, *27*, 202−212.
(74) Liu, L.-Y.; Zhang, X.; Li, H.-X.; Liu, B.; Lang, J.-W.; Kong, L.-B.; Yan, X.-B. Synthesis of Co−Ni oxide microflowers as a superior anode for hybrid supercapacitors with ultralong cycle life. *Chin. Chem. Lett.* **2017**, *28*, 206−212.
(75) Yang, D.; Sun, X.; Lim, K.; Ranganathan Gaddam, R.; Ashok Kumar, N.; Kang, K.; Zhao, X. S. Pre-sodiated nickel cobaltite for high-performance sodium-ion capacitors. *J. Power Sources* **2017**, *362*, 358−365.
(76) Li, S.; Chen, J.; Cui, M.; Cai, G.; Wang, J.; Cui, P.; Gong, X.; Lee, P. S. A High-Performance Lithium-Ion Capacitor Based on 2D Nanosheet Materials. *Small* **2017**, *13*, 1602893.
(77) Peled, E.; Menkin, S. Review—SEI: Past, Present and Future. *J. Electrochem. Soc.* **2017**, *164*, A1703−A1719.
(78) Vaughey, J. T.; Liu, G.; Zhang, J.-G. Stabilizing the surface of lithium metal. *MRS Bull.* **2014**, *39*, 429−435.
(79) Cao, W. J.; Zheng, J. P. Li-ion capacitors with carbon cathode and hard carbon/stabilized lithium metal powder anode electrodes. *J. Power Sources* **2012**, *213*, 180−185.
(80) Aravindan, V.; Ulaganathan, M.; Madhavi, S. Research progress in Na-ion capacitors. *J. Mater. Chem. A* **2016**, *4*, 7538−7548.
(81) Gogotsi, Y. Not just graphene: The wonderful world of carbon and related nanomaterials. *MRS Bull.* **2015**, *40*, 1110−1121.
(82) Zhang, J.; Terrones, M.; Park, C. R.; Mukherjee, R.; Monthioux, M.; Koratkar, N.; Kim, Y. S.; Hurt, R.; Frackowiak, E.; Enoki, T.; et al. Carbon science in 2016: Status, challenges and perspectives. *Carbon* **2016**, *98*, 708−732.

DOI: 10.1021/acs.jpclett.8b01386
J. Phys. Chem. Lett. 2018, 9, 3946−3958